Modified Hybrid Nano Fluid Impact on a MHD Peristaltic wavy Diverging Tube along with connective conditions

Naheeda Iftikhar (naheeda_iftikhar@yahoo.com)
BUITEMS
Hina Sadaf
National University of Sciences and Technology

Research Article

Keywords: Diverging tube, MHD velocity slip, Convective boundary conditions, Modified hybrid nano fluid.

Posted Date: August 3rd, 2022

DOI: https://doi.org/10.21203/rs.3.rs-1908360/v1

Modified Hybrid Nano Fluid Impact on a MHD Peristaltic wavy Diverging Tube along with connective conditions

Naheeda Iftikhar [1], Hina Sadaf [2]

[1]Department of Mathematics, BUITEMS, Quetta, Pakistan

[2] DBS&H, CEME, National University of Sciences and Technology, Islamabad, Pakistan

Abstract

This study focuses our attention towards the peristaltic flow of Zinc, Titanium and Copper modified hybrid nanoparticles, water is occupied as a carrier fluid in a cylindrical diverging tube. The projected model presents the study of MHD, wall properties, slip impact and convective boundary conditions on the flow pattern. The governing partial differential equations and the boundary conditions for computation are evolved by using appropriate transformations. The exact solution for the consequential system of nonlinear differential equations is possible to accomplish using the Cauchy Euler's method. The graphical depiction of velocity and temperature profile using emerging parameters are simulated and examined. The addition of magnetic field in the subjected study shows its distinction in the water flow. Another domain is the addition of heat emission/absorption term in the energy equation to maintain the homogeneous temperature for the water flow. Streamlines pattern is also discussed for modified nano, hybrid nano and nanofluid. We expect the use of these metal nanoparticles in the peristaltic study would be helpful and provide efficient output for drug delivery purposes.

Key Words: Diverging tube, MHD velocity slip, Convective boundary conditions, Modified hybrid nano fluid.

[1] (Corresponding Author), Email: naheeda_iftikhar@yahoo.com. Phone #: +923345897939

Terms and Expressions

$\breve{r}, \breve{z}$	Radial and axial direction in wave frame
$\breve{l}$	Radius of inner tube
$\breve{U}, \breve{W}$	Velocity components in radial and axial direction
$\breve{d}$	Wave speed
λ	Wave length
K	non-uniform parameter
ε	Amplitude ratio
Re	Reynolds's number
L	velocity slip parameter
$c_{\wp}$	Specific heat
$\breve{\mathcal{K}}_{bf}$	Thermal conductivity of base fluid
$\breve{\mathcal{K}}_{nf}$	Thermal conductivity of nanofluid
$\breve{\mathcal{K}}_{hnf}$	Thermal conductivity of hybrid nanofluid
$\breve{\mathcal{K}}_{mhnf}$	Thermal conductivity of Modified hybrid nanofluid
$\breve{\rho}_{nf}$	Density of nanofluid
$\breve{(\rho c_p)}_{nf}$	Heat capacity of nanofluid
$\breve{(\rho c_p)}_{hnf}$	Heat capacity of hybrid nanofluid
$\breve{(\rho c_p)}_{mhnf}$	Heat capacity of Modified hybrid nanofluid
$\breve{\mu}_{nf}$	Dynamic Viscosity of nanofluid
$\breve{\mu}_{hnf}$	Dynamic viscosity of Hybrid nanofluid
$\breve{\mu}_{mhnf}$	Dynamic viscosity of Modified hybrid nanofluid
$\breve{\beta}_{nf}$	Thermal expansion of nanofluid
$\breve{\beta}_{hnf}$	Thermal expansion of Hybrid nanofluid
$\breve{\beta}_{mhnf}$	Thermal expansion of Modified Hybrid nanofluid
$\breve{\sigma}_{nf}$	Electrical conductivity of the nanofluid
$\breve{\sigma}_{hnf}$	Electrical conductivity of Hybrid nanofluid
$\breve{\sigma}_{mhnf}$	Electrical conductivity of Modified hybrid nanofluid
$\breve{\alpha}_{nf}$	Thermal diffusivity of nanofluid
$\breve{\alpha}_{hnf}$	Thermal diffusivity of hybrid nanofluid
$\breve{\alpha}_{mhnf}$	Thermal diffusivity of Modified hybrid nanofluid
$\breve{m}$	Mass per unit area
$\breve{\sigma}$	Elastic tension in the membrane
$\breve{\mathcal{C}}$	Coefficient of viscous damping force
ϕ	Nano particle volume fraction

m	Different shape models
E_1	Rigidity parameter
E_2	Stiffness parameter
E_3	Viscous damping force parameter
M	Hartmann number
$\breve{G_r}$	Grashof number

1. Introduction

The peristaltic mechanism has recently gained particular fame among researchers due to its high demand in the medical and engineering fields. The mechanism involved in peristalsis is almost the same to that of gastrointestinal promotional travels, generally in the colon, and involves the corresponding retrenchment and slackening of the intestinal muscular layer [1]. This is a natural process and is commonly observed in the tract after stimulation. Different parts of human body namely Neurotransmitters and some secretions and the microbiota together perform the complete process. In bypass surgery, this is beneficial for the distribution of blood in the artificial heart and lung. It is also helpful in transporting fluid by preventing fluid contamination. Initially, Latham [2] explained experimentally the movement of fluids via peristalsis. Theoretical addition of Latham with lubrication techniques were made by Shapiro et al. [3]. A number of interesting associated studies are cited in [4-7]. Symmetrical channel has been used to study the peristaltic flow with various thoughts. Physiologists have recently observed that myometrial contraction (flow of intrauterine fluid) symbolized peristalsis, which appear in both symmetrical and asymmetrical channels. These channels can ideally be related to mathematical models of peristaltic flow and same procedure is observed as the fluid moves in a sagittal cross section of the uterus. Furthermore, researchers have shown great attention in studying peristalsis in various configurations with nanofluids. A detailed illustration in this concern is described in Refs. [8–12].

Over the past few decades, the manifestation of MHD theory has widely been observed in numerous engineering and scientific appliances. The above theory is related with the combination of the velocity of the fluid and the magnetic field. The same process is also observed in several problems relating to geophysics and astrophysics. Peristaltic flow with MHD (magneto hydrodynamic) is an interesting field of research because of its huge implementations in physiology and technology. The magnetic field shows the significant role in the design of generators and MHD accelerators, cancer therapy and in the reduction of blood. Another use of magnetic field is in MRI (magnetic resonance imaging), it is used to envision the physiological process in the human flow and brain diagnosis. Sadaf and Nadeem [13] considered the movement of the cilia with heat exchange and the effect of the magnetic field in a curved channel. Lately, in agronomic engineering, the oil industry and the medical field flow of MHD and heat exchange have gotten vital interest. In this context, Davidson, offered numerous applications that have also involved in the field of medicine and engineering, this has brought a tremendous challenge for scientists and engineers. Nowadays, the slip regime has become significant due to its various applications in physiology. The fluid that exhibits slip behavior in peristalsis has significant uses in polishing heart valves, internal cavities, and polymer technology. It is seen in real-world applications that surface moisture is the reason for the fluid that experiences slip behavior on the walls. Bhatti et al [14] studied the slip influence on the peristaltic blood flow taking into account the Jeffery model. Hatami [15] conducted key analysis on the peristaltic movement of the nanofluid and on the heat exchange rate assuming flow conditions in an asymmetrical corrugated channel. Hayat et al. [16] invoked slip effects on the peristalsis of the Jeffery material and also analyzed the impact of entropy generation. Some latest studies in this regime can be followed through [17–21].

The global energy crisis is due to the general increase in growth of the industry and population. Humanitarian disaster is the result of significant development in our society. The consumption of fossil fuels is rapidly increasing, while their availability is steadily declining. Currently, bio renewable energy produced from sustainable means like solar energy, is providing an alter for the diminishing fossils [22].

The bio renewable energy procedure has become an outstanding alternative for energy production. These Solar Systems are designed in such a manner that the system possesses max heat transfer capacity to increase the performance of the appliances. For this purpose, Fluids are helpful that may have the character of increased thermophysical properties. Among these liquids, nanofluids are the best liquids for achieving the liquid's improved heat transfer properties. These liquids refer to fluids in which nanoparticles (NPs) with a particle size in the range of 1 to 100 nm are suspended in a base fluid (water, oil, or organic liquids) [23]. Currently, a brief literature is already available wherein researchers have used nanofluids rather than conventional fluids due to its special properties in absorption refrigeration systems [24], solar cells, solar collectors, and cooling systems as a combination of various solar devices. The nanoparticles are also an option for antimicrobial additives, that opened new ways for cell and particle and can easily facilitate the attraction of the membrane. The main mechanism of nanoparticle toxicity is thought to be through oxidative stress, which damages lipids, carbohydrates, proteins and DNA.

In general, the efficiency of thermal devices ultimately improves because NPs in nanofluids have high density with lower specific heat and these fluids exhibit better convection of heat transfer. The thermal conduction and thermal energy transfer coefficient increases due to the use of nanoliquid. The envision of adding nanoparticles to the classical fluid was first practically applied by Choi and Eastman [25]. Cho [26] experimentally studied the turbulent thermal energy transport of water with addition of titanium dioxide and γ-alumina (Al2O3). Authors ensued that the mixture of nanoparticles with water precipitation improves the coefficient of transformation of thermal energy by convection. More significant research on this area can be found from references [27–29].

Benefits of hybrid nanoliquid and their applications in different fields are scrutinized and discussed by many authors. Suresh et al. [30] analyzed Copper with alumina NPs by using the two-step method. Another study by Hayat and Nadeem [31] discussed the properties of thermal energy transfer of the Ag-CuO while considering water as a base fluid. Their results also proven the strength of hybrid nanofluid in contrary to the conventional nanofluid. Safaei et al. [32] examined the effects on the thermal conduction of $ZnOTiO_2$/EG hybrid nanofluid by applying the firing technique and the artificial neural network. The thermal efficiency of nanocomposites is believed to be determined by the impact of including the heat capacity and thermal capacity of the base fluid, the flow rate, the solubility of the nanofluid, the amount of colloidal matter, as well as their proportions and the structure of the flow. Scientists have tried to find new means to enhance the efficiency of the system. Sulochana and Ashwinkumar [33] exhibited the convective flow of nanofluid by taking into account the influences of Brownian motion and the effects of thermophoresis.

As we have considered Zinc, copper and titanium modified hybrid nanoparticles in this manuscript because of their applications in different fields. Few are explained as under: -

Zinc, Titanium and Copper has many commonly applications as three metals have different benefits. Although, zinc is brittle and weak but is fruitful for electroplating. To counter this deficiency, Titanium is used as alloy because Titanium is comparatively strong and corrosion-resistant material. Apart from Zinc and Titanium, Copper is used to enhance conductivity of the metals and is also used as base metal because of its improved elasticity, flexibility, hardness, colour, and resistance to corrosion.

This manuscript is an endeavour to discuss the peristaltic motion in modified hybrid nanofluid with MHD. Apart from this, convective heat transfer, wall properties and slip effects are also considered. In this manuscript, Navier Stock's equations has been solved by keeping in view the flow assumptions using exact technique. Graphical and tabulated description has also been used to explain physical effects involving parameters i.e. velocity slip, convective heat transfers and solid nanoparticle.

As a result, the manuscript has been modelled and analysed by assuming the

(i) diverging horizontal tube $\breve{R_2} = \breve{H} = \breve{l}(\breve{Z}) + \breve{b} \sin\frac{2\pi}{\lambda}\left(\breve{Z} - \breve{d}\breve{t}\right)$.

(ii) Incompressible, electrically conducting viscous fluid for the study of 2-D peristaltic flow with magneto-hydrodynamics and Sinusoidal waves propagating along the direction of flow.

(iii) Cylindrical coordinates $\left(\breve{r}, 0, \breve{z}\right)$ are considered for the modeling of flow equations and modified with the postulation of large wavelength and small Reynolds number.

(iv) Metal of Zinc, copper and Titanium are considered as modified hybrid nanoparticles are distributed uniformly in the diverging horizontal tube.

(v) Water is taken as a base fluid.

(vi) (Zinc, copper and Titanium) nanoparticles and water fluid are locally in the thermal stability.

(vii) Wall properties, convective boundary conditions, slip, and various shape effects are used as assumptions.

(viii) In the best interests of the above flow theory, the governing equations can be recoiled as Equations (1–14).

The Hamilton-Crosser model is anticipated to study the thermal conductivity effects on the modified hybrid nanofluid. In view of above considerations, the modelled governing equations are suitable to attain the analytical solution of the formulated modified hybrid nanoparticles problem. These solutions comprise the temperature, velocity and hence stream function are obtained. The inspiration of the working parameters on flow of fluid and heat transfer characteristics are specifically described. Their effects are also graphically signified and discussed in detail. The practical manifestation of same is expected to be useful in colloidal drug delivery systems.

1. Problem Statement

The flow is assumed in 2-D and $\boldsymbol{B}$ = (Bo, 0, 0) is the representation of magnetic field that is working in the radial direction. An additional feature of radiation in energy calculations is occupied along the radial track as a one-dimensional heat flux.

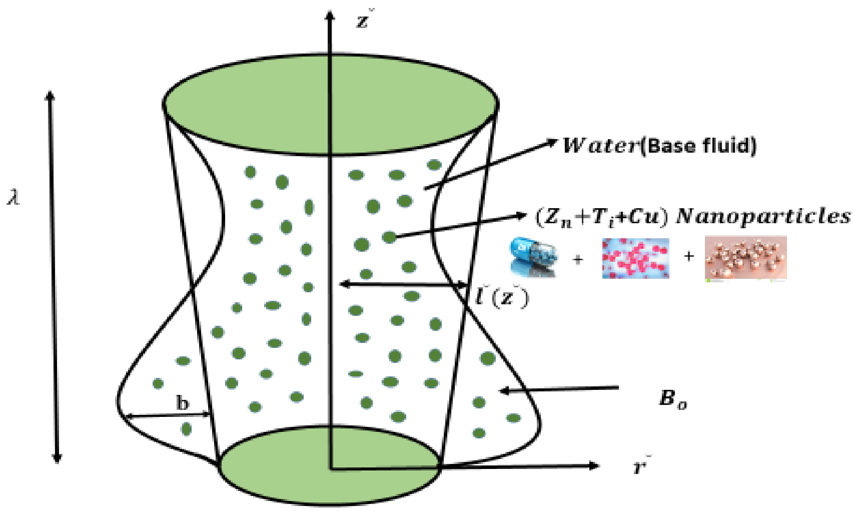

Fig 1.

Flow Geometry

$\breve{R} = \breve{H}$ is signifies as the wall of the tube and $\breve{T_0}$ assigns as the magnitude for temperature $\breve{T}$ at this wall. Although, the flow equations (1-4) along modified hybrid nanoparticles and MHD can be followed as:

$$\frac{\partial \breve{\mathcal{U}}}{\partial \breve{\mathcal{R}}} + \frac{\partial \breve{\mathcal{W}}}{\partial \breve{\mathcal{Z}}} + \frac{\breve{\mathcal{U}}}{\breve{\mathcal{R}}} = 0 \quad (1)$$

$$\breve{\rho}_{mhnf}\left[\frac{\partial \breve{\mathcal{U}}}{\partial \breve{t}} + \breve{\mathcal{U}}\frac{\partial \breve{\mathcal{U}}}{\partial \breve{\mathcal{R}}} + \breve{\mathcal{W}}\frac{\partial \breve{\mathcal{U}}}{\partial \breve{\mathcal{Z}}}\right] = -\frac{\partial \breve{\mathcal{P}}}{\partial \breve{\mathcal{R}}} + \breve{\mu}_{mhnf}\left[\frac{1}{\breve{\mathcal{R}}}\frac{\partial}{\partial \breve{\mathcal{R}}}\left(\breve{\mathcal{R}}\frac{\partial \breve{\mathcal{U}}}{\partial \breve{\mathcal{R}}}\right) + \frac{\partial^2 \breve{\mathcal{U}}}{\partial \breve{\mathcal{Z}}^2} - \frac{\breve{\mathcal{U}}}{\breve{\mathcal{R}}^2}\right] \quad (2)$$

$$\breve{\rho}_{mhnf}\left[\frac{\partial \breve{\mathcal{W}}}{\partial \breve{t}} + \breve{\mathcal{U}}\frac{\partial \breve{\mathcal{W}}}{\partial \breve{\mathcal{R}}} + \breve{\mathcal{W}}\frac{\partial \breve{\mathcal{W}}}{\partial \breve{\mathcal{Z}}}\right] = -\frac{\partial \breve{\mathcal{P}}}{\partial \breve{\mathcal{Z}}} + \breve{\mu}_{mhnf}\left[\frac{1}{\breve{\mathcal{R}}}\frac{\partial}{\partial \breve{\mathcal{R}}}\left(\breve{\mathcal{R}}\frac{\partial \breve{\mathcal{W}}}{\partial \breve{\mathcal{R}}}\right) + \frac{\partial^2 \breve{\mathcal{W}}}{\partial \breve{\mathcal{Z}}^2}\right] + (\rho\beta)\breve{}_{nf}\, g\left(\mathcal{T} - \breve{\mathcal{T}_o}\right) - \frac{\sigma_{mhnf}}{\sigma_{bf}}\frac{B_o^2}{\breve{\mathcal{R}}^2}\breve{\mathcal{W}} \quad (3)$$

The energy equation is

$$\left(\rho c_p\right)\breve{}_{mhnf}\left[\frac{\partial \breve{\mathcal{T}}}{\partial \breve{t}} + \breve{\mathcal{U}}\frac{\partial \breve{\mathcal{T}}}{\partial \breve{\mathcal{R}}} + \breve{\mathcal{W}}\frac{\partial \breve{\mathcal{T}}}{\partial \breve{\mathcal{Z}}}\right] = \breve{\mathcal{K}}_{mhnf}\left[\frac{\partial^2 \breve{\mathcal{T}}}{\partial \breve{\mathcal{R}}^2} + \frac{1}{\breve{\mathcal{R}}}\frac{\partial \breve{\mathcal{T}}}{\partial \breve{\mathcal{R}}} + \frac{\partial^2 \breve{\mathcal{T}}}{\partial \breve{\mathcal{Z}}^2}\right] + \breve{Q_o} \quad (4)$$

In the above calculations $\breve{\rho}_{mhnf}$ is density of modified hybrid nanofluid, $\breve{\mathcal{U}}$ and $\breve{\mathcal{W}}$ are the suitable velocity units in radial and axial directions. The thermophysical properties for nanofluid, hybrid nanofluid, and modified nanofluid are expressed in Table 1. [34]:-

To investigate the convective boundary conditions of modified nanofluids, this test is familiar with anomalous types of physical properties. The modified nanofluid is examined by taking a combination of Zn, Ti and Cu with the base fluid water.

The nanoparticles concentration of Zn, Ti and Cu are $(0.05 \leq \emptyset_1 \leq 0.09, 0.05 \leq \emptyset_2 \leq 0.09$ and $0.05 \leq \emptyset_3 \leq 0.09$). To make it ideal, the final strong thermophysical properties of $(Zn\,/\,water)$ nanofluids, $(Zn - Ti\,/\,water)$ hybrid nanofluids, and $(Zn - Ti - Cu\,/\,water)$ modified nanofluids are in Table 1. While m is for shape factor.

Table 1.

Properties	Nanofluid
Thermal Diffusivity	$\breve{\alpha}_{nf} = \frac{\breve{k}_{nf}}{(\rho c_p)^*_{nf}}$,
Viscosity	$\breve{\mu}_{nf} = \frac{\breve{\mu}_{bf}}{(1-\varphi_1)^{2.5}}$,
Electrical conductivity	$\breve{\sigma}_{nf} = \breve{\sigma}_{bf}\left[\frac{(\sigma_{s1} + 2\breve{\sigma}_{bf}) - 2\varphi_1(\breve{\sigma}_{bf} - \sigma_{s1})}{(\sigma_{s1} + 2\breve{\sigma}_{bf}) + \varphi_1(\breve{\sigma}_{bf} - \sigma_{s1})}\right]$,
Thermal conductivity	$\frac{\breve{k}_{nf}}{\breve{k}_{bf}} = \frac{\breve{k}_{s1}+(m-1)\breve{k}_{bf}-(m-1)(\breve{k}_{bf}-\breve{k}_{s1})\varphi_1}{\breve{k}_{s1}+(m-1)\breve{k}_{bf}+(\breve{k}_{bf}-\breve{k}_{s1})\varphi_1}$,
Density	$\breve{\rho}_{nf} = \breve{\rho}_{bf}(1-\varphi_1) + \varphi_1\breve{\rho}_{s1}$,
Heat capacity	$\breve{(\rho c_p)}_{nf} = \left[(1-\varphi_1)\breve{(\rho c_p)}_{f} + \varphi_1\breve{(\rho c_p)}_{s1}\right]$,
Thermal expansion	$\breve{(\rho\beta)}_{nf} = \breve{(\rho\beta)}_{f}\left[(1-\varphi_1) + \varphi_1\left(\breve{(\rho\beta)}_{s1}/\breve{(\rho\beta)}_{bf}\right)\right]$
Properties	**Hybrid Nanofluibd**
Thermal Diffusivity	$\breve{\alpha}_{hnf} = \frac{\breve{k}_{hnf}}{\breve{(\rho c_p)}_{hnf}}$,
Viscosity	$\breve{\mu}_{hnf} = \frac{\breve{\mu}_{f}}{(1-\varphi_2)^{2.5}(1-\varphi_1)^{2.5}}$,
Electrical conductivity	$\breve{\sigma}_{hnf} = \breve{\sigma}_{bf}\left[\frac{(\sigma_{s2} + 2\breve{\sigma}_{nf}) - 2\varphi_2(\breve{\sigma}_{nf} - \sigma_{s2})}{(\sigma_{s2} + 2\breve{\sigma}_{nf}) + \varphi_2(\breve{\sigma}_{nf} - \sigma_{s2})}\right]$, where $\breve{\sigma}_{nf} = \breve{\sigma}_{bf}\left[\frac{(\sigma_{s1}+2\breve{\sigma}_{bf})-2\varphi_1(\breve{\sigma}_{bf}-\sigma_{s1})}{(\sigma_{s1}+2\breve{\sigma}_{bf})+\varphi_1(\breve{\sigma}_{bf}-\sigma_{s1})}\right]$,
Thermal conductivity	$\frac{\breve{k}_{hnf}}{\breve{k}_{nf}} = \frac{\breve{k}_{s2}+(m-1)\breve{k}_{nf}-(m-1)(\breve{k}_{nf}-\breve{k}_{s2})\varphi_2}{\breve{k}_{s2}+(m-1)\breve{k}_{nf}+(\breve{k}_{nf}-\breve{k}_{s2})\varphi_2}$, Where $\frac{\breve{k}_{nf}}{\breve{k}_{bf}} = \frac{\breve{k}_{s1}+(m-1)\breve{k_{bf}}-(m-1)(k_{bf}-\breve{k}_{s1})\varphi_1}{\breve{k}_{s1}+(m-1)\breve{k_{bf}}+(\breve{k_{bf}}-\breve{k}_{s1})\varphi_1}$,
Density	$\breve{\rho}_{hnf} = \breve{\rho}_{bf}\left[(1-\varphi_1)(1-\varphi_2) + \varphi_1\left(\breve{\rho}_{s1}/\breve{\rho}_{bf}\right)\right] + \varphi_2\breve{\rho}_{s2}$,
Heat capacity	$\breve{(\rho c_p)}_{hnf} = \left[(1-\varphi_2)(1-\varphi_1)\breve{(\rho c_p)}_{f} + \varphi_1\breve{(\rho c_p)}_{s1}\right] + \varphi_2\breve{(\rho c_p)}_{s2}$,
Thermal expansion	$\breve{(\rho\beta)}_{hnf} = \breve{(\rho\beta)}_{f}(1-\varphi_2)\left[(1-\varphi_1) + \varphi_1\left(\breve{(\rho\beta)}_{s1}/\breve{(\rho\beta)}_{f}\right)\right] + \varphi_2\breve{(\rho\beta)}_{s2}$
Properties	**Modified Hybrid Nanofluid**

Thermal Diffusivity	$\breve{\alpha}_{mhnf} = \frac{\breve{k}_{mhnf}}{\breve{(\rho c_p)}_{mhnf}},$
Viscosity	$\breve{\mu}_{mhnf} = \frac{\breve{\mu}_{bf}}{(1-\varphi_3)^{2.5}(1-\varphi_2)^{2.5}(1-\varphi_1)^{2.5}},$
Electrical conductivity	$\breve{\sigma}_{mhnf} = \breve{\sigma}_{hnf}\left[\frac{\sigma_{s3} + 2\breve{\sigma}_{hnf} + 2\varphi_3(\breve{\sigma}_{hnf} - \sigma_{s3})}{\sigma_{s3} + 2\breve{\sigma}_{hnf} + \varphi_3(\breve{\sigma}_{hnf} - \sigma_{s3})}\right],$
Thermal conductivity	$\frac{\breve{k}_{mhnf}}{\breve{k}_{hnf}} = \frac{\breve{k}_{s3}+(m-1)\breve{k}_{nf}-(m-1)(\breve{k}_{nf}-\breve{k}_{s3})\varphi_3}{\breve{k}_{s3}+(m-1)\breve{k}_{nf}+(\breve{k}_{nf}-\breve{k}_{s3})\varphi_3},$ Where $\frac{\breve{k}_{hnf}}{\breve{k}_{nf}} = \frac{\breve{k}_{s2}+(m-1)\breve{k}_{nf}-(m-1)(\breve{k}_{nf}-\breve{k}_{s2})\varphi_2}{\breve{k}_{s2}+(m-1)\breve{k}_{nf}+(\breve{k}_{nf}-\breve{k}_{s2})\varphi_2},$
Density	$\breve{\rho}_{mhnf} = (1-\varphi_3)\left[(1-\varphi_2)(1-\varphi_1)\breve{\rho}_{bf} + \varphi_1\breve{\rho}_{s1} + \varphi_2\breve{\rho}_{s2}\right] + \varphi_3\breve{\rho}_{s3},$
Heat capacity	$\breve{(\rho c_p)}_{mhnf} = (1-\varphi_3)\left[\left((1-\varphi_2)(1-\varphi_1)\breve{(\rho c_p)}_{bf} + \varphi_1\breve{(\rho c_p)}_{s1}\right) + \varphi_2\breve{(\rho c_p)}_{s2}\right] + \varphi_3\breve{(\rho c_p)}_{s3},$
Thermal expansion	$\breve{(\rho\beta)}_{mhnf} = (1-\varphi_3)\left[(1-\varphi_1)(1-\varphi_2)\breve{(\rho\beta)}_{bf} + \varphi_1\breve{(\rho\beta)}_{s1} + \varphi_2\breve{(\rho\beta)}_{s2}\right] + \varphi_3\breve{(\rho\beta)}_{s3}$

Table 2.

Nanoparticles & shape factor (m)	Platelets (5.7)	Cylinders (4.9)	Bricks (3.7)
		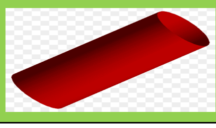	

2. Methodology

The apt boundary conditions are expressed in eq. (5-6) according to the physical happening (shown in Fig. 1).

$$\frac{\partial \breve{w}}{\partial \breve{r}} = 0, at\ \breve{\mathcal{R}} = 0$$

$$\breve{\mathcal{W}} - \breve{\mathcal{W}}_{\mathcal{W}} = -L^{*}\tau_{\breve{\mathcal{R}}\breve{Z}}, at\ \breve{\mathcal{R}} = \breve{H} \quad (5)$$

$$\frac{\partial \breve{\theta}}{\partial \breve{r}} = 0, at\ \breve{\mathcal{R}} = 0$$

$$\eta(\mathcal{T}-\breve{\mathcal{T}}_0) = -\breve{\mathcal{K}}_{mhnf}\frac{\partial \breve{\mathcal{T}}}{\partial \breve{\mathcal{R}}}, at\ \breve{\mathcal{R}} = \breve{H} \tag{6}$$

Here $\breve{\mathcal{W}}$ is the velocity of fluid. The fundamental equation for the flow of flexible wall is explained as:

$$\breve{L}(\breve{\mathcal{H}}) = (\breve{\mathcal{P}} - \breve{\mathcal{P}_0}) \tag{7}$$

Where $\breve{L}$ is an operator that categorized the motion of stretched damping forces membrane while the pressure $\breve{\mathcal{P}_0}$ is due to the tension in the muscle acting on the outer surface of the wall which is assumed to be zero. So $\breve{L}$ can be written as

$$\breve{L} = -\breve{\sigma}\frac{\partial^2}{\partial \breve{Z}^2} + \breve{m}\frac{\partial^2}{\partial \breve{t}^2} + \breve{C}\frac{\partial}{\partial \breve{t}} \tag{8}$$

Where $\breve{\sigma}$ shows elastic tension in the membrane, $\breve{m}$ represents mass per unit area, $\breve{C}$ is coefficient of viscous damping forces.

Following are the non-dimensional parameters are used to linearize the equations:

$$\breve{r} = \frac{\breve{\mathcal{R}}}{\breve{\ell_2}}, \breve{Z} = \frac{\breve{Z}}{\lambda}, \breve{u} = \frac{\lambda\breve{\mathcal{U}}}{\breve{\ell_2}\breve{d}}, \breve{w} = \frac{\breve{W}}{\breve{d}}, \varepsilon = \frac{b}{\breve{\ell_2}}, \breve{P} = \frac{\breve{\mathcal{P}}\breve{\ell_2}^2}{\lambda\breve{\mu}_{f}\breve{d}}, t = \frac{c\breve{t}}{\lambda},$$

$$Re = \frac{\breve{\rho}_{f}\breve{\ell_2}\breve{d}}{\breve{\mu}_{f}}, \breve{\theta} = \frac{\mathcal{T}-\breve{\mathcal{T}}_o}{\breve{\mathcal{T}}_o}, \tau = \frac{\breve{\ell_2}\breve{\tau}}{\breve{d}\mu_0}, \breve{B} = \frac{Q_o\breve{\ell_2}^2}{(\mathcal{T}-\breve{\mathcal{T}}_o)\breve{k}_{bf}}, G_r = \frac{(\mathcal{T}-\breve{\mathcal{T}}_o)g\beta_f\rho_f\breve{\ell_2}^2}{\breve{\mu}_{f}\breve{d}}$$

$$M^2 = \frac{\breve{\sigma}_{f}{B_0}^2\breve{\ell_2}}{\breve{\mu}_{f}}, \breve{E_1} = \frac{\breve{\sigma}\breve{\ell_2}^3}{\lambda^3\breve{d}\breve{\mu}_{f}}, \breve{E_2} = \frac{\breve{m}\breve{\ell_2}^3\breve{d}}{\lambda^3\breve{\mu}_{f}}, \breve{E_3} = \frac{\breve{\ell_2}^3\breve{d}}{\lambda^2\breve{\mu}_{f}}, \quad L = \frac{L^*\breve{\mu}_{f}}{\breve{\ell_2}} \tag{9}$$

$$\ell(\breve{Z}) = \breve{\ell}_2 + K\breve{Z}, h = \frac{\breve{h}}{\breve{\ell_2}} = 1 + \frac{\lambda K\breve{Z}}{\breve{\ell}_2} + \varepsilon\sin 2\pi(\breve{Z} - \breve{t}),$$

In constraint cases $R_e \rightarrow 0$. the inertial flow communicates to a longitudinal velocity shape. In the laboratory frame, the pressure gradient depends only on $\breve{z}$ and $\breve{t}$ because there is no streamline curvature to turn out a pressure gradient in the transverse conduct when $\delta \longrightarrow 0$. As a result, it is possible to use a long length and a small number of Reynold's, which shows $\delta \rightarrow 0$.and $R_e \rightarrow 0$. This scheme was realistic by Shapiro [3] to the portrayal of chyme passage in the male small intestine. Employing the conditions of large wavelength observe that $\delta \rightarrow 0$ and $Re \longrightarrow 0$ negates convective inertial forces. Execution of these guesses to Eq. (1) -(6) results

$$\frac{\partial \breve{\mathcal{P}}}{\partial \breve{r}} = 0 \tag{10}$$

$$-\frac{\partial \breve{\mathcal{P}}}{\partial \breve{Z}} + \frac{\breve{\mu}_{mhnf}}{\breve{\mu}_{bf}}\left[\frac{1}{\breve{r}}\frac{\partial}{\partial \breve{r}}\left(\breve{r}\frac{\partial \breve{W}}{\partial \breve{r}}\right)\right] + \frac{\breve{(\rho\beta)}_{mhnf}}{\breve{(\rho\beta)}_{bf}}G_r\breve{\theta} - F\frac{M^2}{\breve{r}^2}\breve{\mathcal{W}} = 0 \tag{11}$$

$$\breve{k}_{mhnf}\left[\frac{1}{\breve{r}}\frac{\partial \breve{\theta}}{\partial \breve{r}}+\frac{\partial^2 \breve{\theta}}{\partial \breve{r}^2}\right]+\breve{B}\breve{k}_{bf}=0 \tag{12}$$

After dimensionless eq. 8 becomes:

$$\frac{\partial \breve{\mathcal{P}}}{\partial \breve{Z}}=\frac{\partial \breve{L}(h)}{\partial \breve{Z}}= \breve{E}_1\frac{\partial^3 h}{\partial \breve{Z}^3}+\breve{E}_2\frac{\partial^3 h}{\partial \breve{Z}^2\partial t}+\breve{E}_3\frac{\partial^2 h}{\partial \breve{Z}\partial t} \tag{13a}$$

By means of boundary constraint dependable with the geometry are:-

$$\frac{\partial \breve{\theta}}{\partial \breve{r}}=0 \quad at \quad \breve{r}=0$$

$$\breve{\gamma}\breve{\theta}+\frac{\partial \breve{\theta}}{\partial \breve{r}}=0 \ \ at\ \breve{r}=h \tag{13b}$$

Where $\breve{\gamma}=\frac{\breve{\mathcal{K}}_{bf}B_i}{\breve{\mathcal{K}}_{mhnf}}$, $\quad B_i=\frac{l_2\eta}{\breve{\mathcal{K}}_{bf}}$

$$\frac{\partial \breve{w}}{\partial \breve{r}}=0 \ \ at\ \breve{r}=0$$

$$\breve{w}+LA\frac{\partial \breve{w}}{\partial \breve{r}}=0 \ \ at\ \breve{r}=h \tag{13c}$$

Numerical values are apt in Table 1[20].

Physical properties	**Zinc**	**Copper**	**Titanium**	**Water**
Heat capacity (J/kgk)	389	385	522	4179
Density(kg/m^3)	7140	8933	4500	997.1
Thermal conductivity(w/m)	99.2	116	401	0.613
Electrical conductivity(s/m)	1.69×10^7	5.96×10^7	2.38×10^6	5.5×10^{-6}
Thermal expansion$(1/k)$	39.7×10^{-6}	16.8×10^{-6}	7.14×10^{-6}	7.03×10^{-6}

3. Techniques

Exact solution is required for temperature so, By using Eq. 13c we will get the solution

$$\breve{\theta}=\frac{-\breve{B}\mathcal{S}\breve{r}^2}{4Y}+D_1\log\breve{r}+D_2$$

$$\breve{\theta}=\left[-\frac{\breve{B}\mathcal{S}\breve{r}^4}{4Y}+\frac{\breve{B}\mathcal{S}h\breve{r}^2}{2Y}+\frac{\breve{B}\mathcal{S}\breve{\gamma}\breve{r}^2\breve{h}^2}{4Y}\right] \tag{14}$$

By substituting above solution in eq. 11 we will get the eqn.

$$\breve{r}^2 \frac{d^2 \breve{w}}{d\breve{r}^2} + \breve{r}\frac{d\breve{w}}{d\breve{r}} - \frac{FM^2}{A}\breve{w} = \frac{\breve{r}^2}{A}\frac{dp}{dz} - \frac{T}{A}G_r\left[-\frac{\breve{B}\breve{S}\breve{r}^4}{4Y} + \frac{\breve{B}\breve{S}h\breve{r}^2}{2Y} + \frac{\breve{B}\breve{S}\gamma\breve{r}^2\breve{h}^2}{4Y}\right] \tag{15}$$

Where $A = \frac{\breve{\mu}_{mhnf}}{\breve{\mu}_{bf}}$, $F = \frac{\breve{\sigma}_{mhnf}}{\breve{\sigma}_{bf}}$, $T = \frac{\breve{(\rho\beta)}_{mhnf}}{\breve{(\rho\beta)}_{bf}}$, $S = \breve{k}_{bf}$ and $Y = \breve{k}_{mhnf}$

The general form of the solution is

$$\breve{w} = C_1(\breve{r})^{-\breve{\mathcal{M}}\sqrt{F/A}} + C_2(\breve{r})^{\breve{\mathcal{M}}\sqrt{F/A}} + \frac{\left(\frac{d\breve{p}}{d\breve{z}}\right)}{A}\left(\frac{(\breve{r})^2}{4-\frac{FM^2}{A}}\right) - \frac{T}{A}G_r\left[-\frac{\breve{B}\breve{S}(\breve{r})^4}{4Y\left(16-\frac{FM^2}{A}\right)} + \frac{\breve{B}\breve{S}\breve{h}(\breve{r})^2}{2Y\left(4-\frac{FM^2}{A}\right)} + \frac{\breve{B}\breve{S}\gamma(\breve{r})^2\breve{h}^2}{4Y\left(4-\frac{FM^2}{A}\right)}\right] \tag{16}$$

By using eq. (13c) we obtained C_1 *and* C_2 as under:-

$$C_1 = \left[\begin{array}{l} \frac{-\breve{h}^2}{A}\frac{d\breve{P}/d\breve{z}}{\left(16-\frac{FM^2}{A}\right)} + \frac{T}{A}G_r\left(\frac{-\breve{B}\breve{S}\breve{h}^4}{4Y\left(16-\frac{FM^2}{A}\right)} + \frac{\breve{B}\breve{S}\breve{h}^3}{2Y\left(4-\frac{FM^2}{A}\right)} + \frac{\breve{B}\breve{S}\gamma\breve{h}^4}{4Y\left(4-\frac{FM^2}{A}\right)}\right) \\ -\frac{2\breve{h}}{A}\frac{\left(\frac{d\breve{p}}{d\breve{z}}\right)LA^*}{\left(16-\frac{FM^2}{A}\right)} + \frac{T}{A}LA^*G_r\left[-\frac{\breve{B}\breve{S}\breve{h}^3}{Y\left(16-\frac{FM^2}{A}\right)} + \frac{\breve{B}\breve{S}\breve{h}^2}{Y\left(4-\frac{FM^2}{A}\right)} + \frac{\breve{B}\breve{S}\gamma\breve{h}^3}{2Y\left(4-\frac{FM^2}{A}\right)}\right] \end{array}\right]$$

$C_2 = 0$

Stream function expression can be expressed as

$$\breve{u} = -\frac{1}{\breve{r}}\frac{\partial\psi}{\partial\breve{Z}}, \quad \breve{w} = \frac{1}{\breve{r}}\frac{\partial\psi}{\partial\breve{Z}} \quad \text{at} \quad \breve{r} = h = \breve{r}_2 \tag{17}$$

Expression of heat transfer for the walls is conveyed as:

$$Z_2 = \left(\frac{\partial\breve{\theta}}{\partial\breve{r}}\right)\left(\frac{\partial h}{\partial\breve{z}}\right) \quad at\ \breve{r} = \breve{r}_2 \tag{18}$$

$\breve{r}$	Z_2 *for Bi=1.0* **(Zn-Ti -Cu)/H_2O**	Z_2 *for Bi=1.1* **(Zn-Ti-Cu)/H_2O**	Z_2 *for Bi=1.2* **(Zn-Ti-Cu)/H_2O**	Z_2 *for Bi=1.0* **(Zn-Ti)/H_2O**	Z_2 *for Bi=1.1* **(Zn-Ti)/H_2O**	Z_2 *for Bi=1.2* **(Zn-Ti)/H_2O**	Z_2 *for Bi=1.0* **(Zn)/H_2O**	Z_2 *for Bi=1.1* **(Zn)/H_2O**	Z_2 *for Bi=1.2* **(Zn)/H_2O**
-1.02	-4.92425	-4.92425	-4.92425	-5.79232	-5.79232	-5.79232	-7.15205	-7.15205	-7.15205
-0.92	-4.62628	-4.62628	-4.62628	-5-55876	-5.55876	-7.12488	-7.01935	-7.01935	-7.01935
-0.82	-5.01427	-5.01427	-5.01427	-6.0677	-6.0677	-9.44816	-7.71774	-7.71774	-7.71774
-0.72	-5.94013	-5.94013	-5.94013	-7.12488	-7.12488	-6.6842	-8.98061	-8.98061	-8.98061
-0.62	-7.05032	-7.05032	-7.05032	-8.3266	-8.3266	-6.07174	-10.3257	-10.3257	-10.3257
-0.52	-7.92429	-7.92086	-7.92086	-9.21397	-9.21397	-9.21793	-11.2395	-11.2395	-11.2395
-0.42	-8.21936	-8.21936	-9.44816	-9.44816	-9.44816	-9.44816	-11.3729	-11.3729	-11.37294
-0.32	-7.8319	-7.8319	-8.93986	-8.93986	-8.93986	-10.6753	-10.6753	-10.6753	-10.6753
-0.22	-6.90661	-6.90661	7.88336	-7.88336	-7.88336	-9.41332	-9.41332	-9.41332	-9.41332
-0.12	-5.79708	-5.79708	-6.6824	-6.6824	-6.6824	-8.06915	-8.06915	-8.06915	-8.06915
-0.02	-4.92725	-4.92725	-5.79587	-5.79587	-5.79587	7.15646	-7.15646	-7.15646	-7.15646

0.08	-4.62951	-4.62951	-5.56256	-5.56256	-5.56256	-7.02406	-5.56256	-7.02406	-7.02406
0.18	-5.01773	-5.01773	-6.07174	-6.07174	-6.07174	-7.7227	-6.07174	-7.7227	-7.7227
0.28	-5.94372	-5.94372	-7.12904	-7.12904	-7.122904	-8.98569	-8.98569	-8.98569	-8.98569
0.38	-7.05389	-7.05389	-8.33074	-8.33074	-8.33074	-10.3307	-10.3307	-10.3307	-10.3307
0.48	-7.92429	-7.92429	-9.21793	-9.21793	-9.21793	-11.2442	-11.2442	-11.2442	-11.2442
0.58	-8.22255	-8.22255	-9.45187	-9.45187	-9.45187	-11.3774	-11.3774	-11.3774	-11.3774
0.68	-7.83487	-7.83487	-8.94332	-8.94332	-8.94332	-10.6796	-10.6796	-10.6796	-19.6796
0.78	-6.90945	-6.90945	-7.88671	-7.88671	-7.88671	-9.41744	-9.41744	9.41744	-9.41744
0.88	-5.79993	-5.79993	-6.68577	-6.68577	-6.68577	-8.07334	-8.07334	-8.07334	-8.07334
0.98	-4.93024	-4.93024	-5.79942	-5.79942	-5.79942	-7.16087	-7.16087	-7.16087	-7.16087

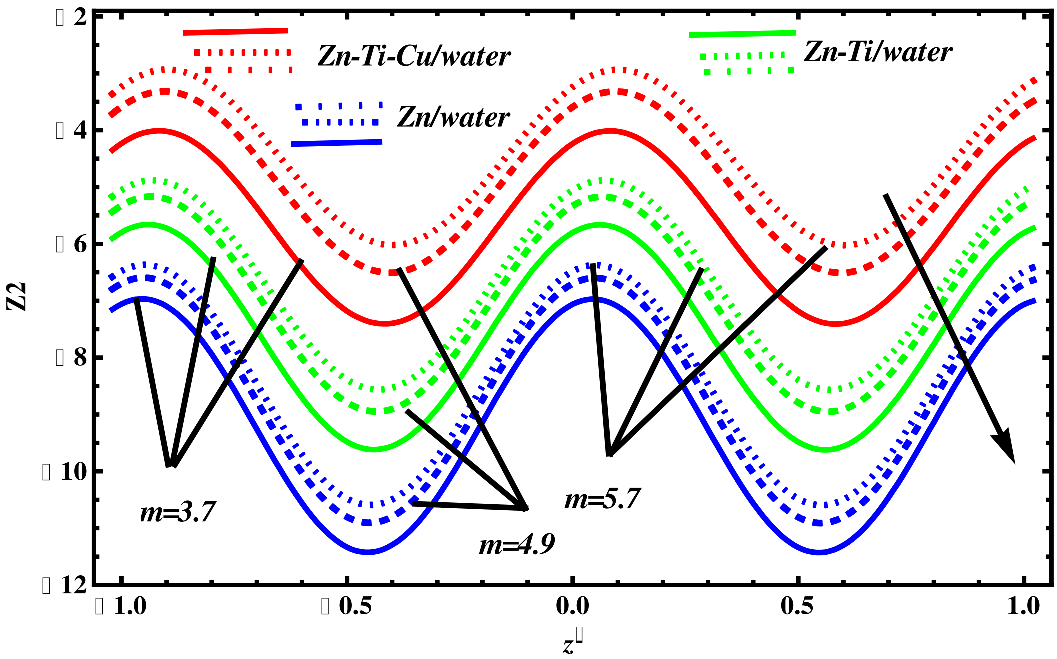

Fig 2

B=0.01, B_i=1.0, ϵ=0.2, $\boldsymbol{\lambda = 0.01}$

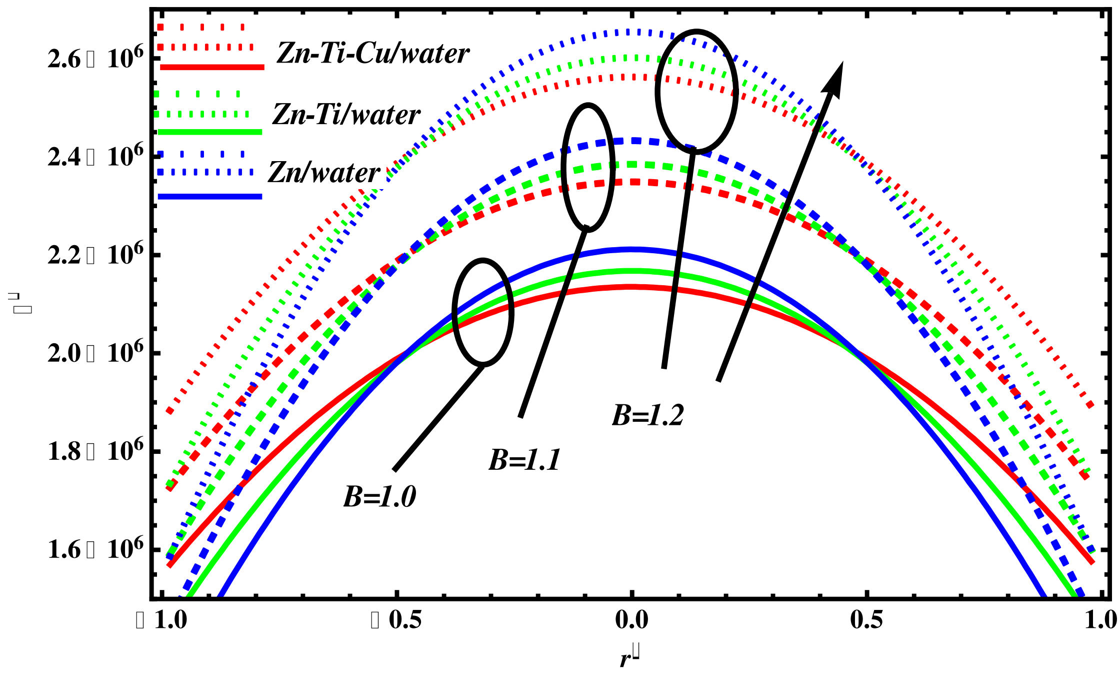

Fig 2(a)

$\mathcal{Z}\breve{} = 0.1, \mathrm{m} = 3.7, \mathrm{k} = 0.1, = 0.01, \mathrm{Bi} = 0.1$

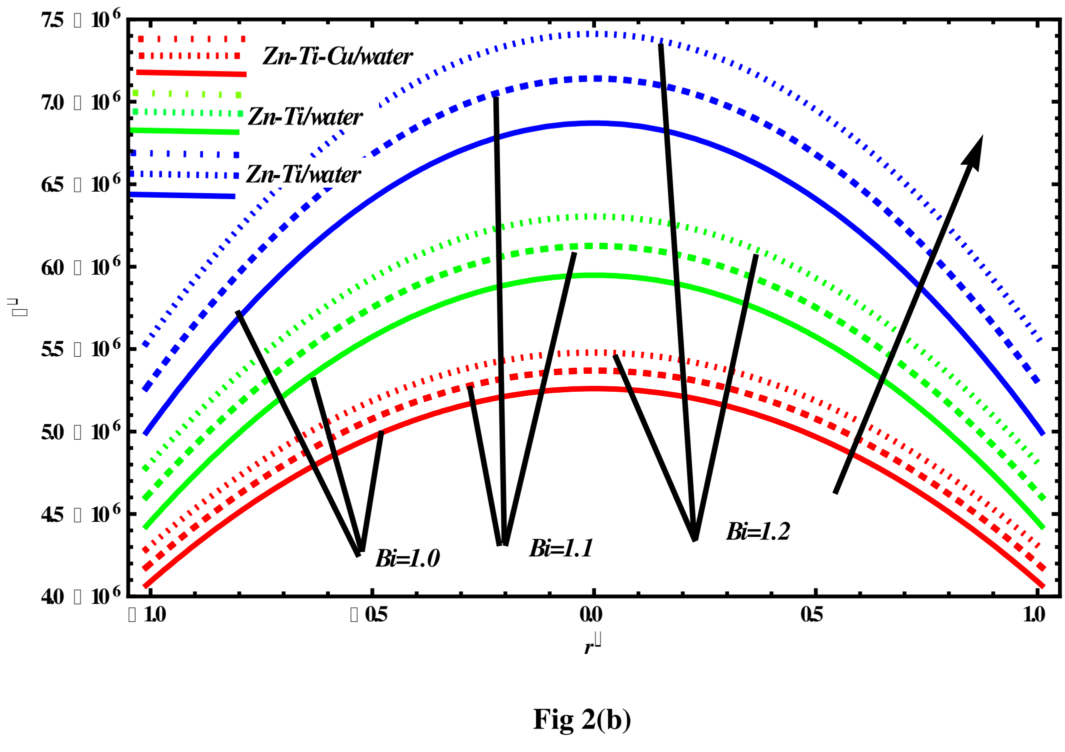

Fig 2(b)

$\mathcal{Z}\breve{}$=0.1, m=3.7, k=0.1, λ =0.01, B=2

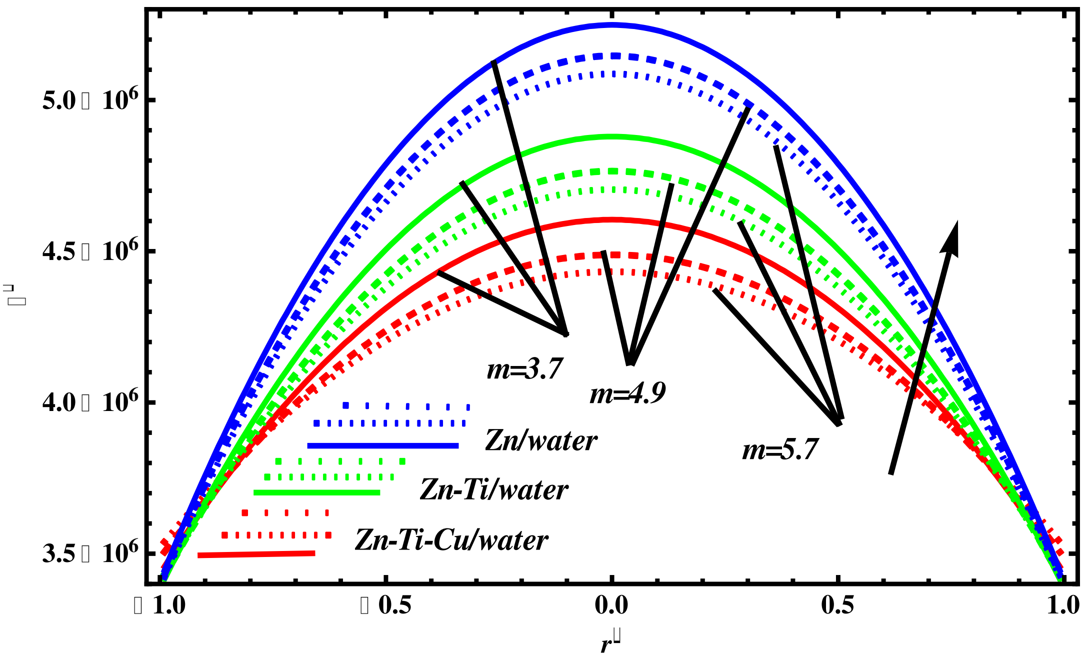

Fig 2(c)

$\mathcal{Z}$˘=0.1, k=0.1, $\boldsymbol{\lambda}$ =0.01, B_i=0.4, B=2

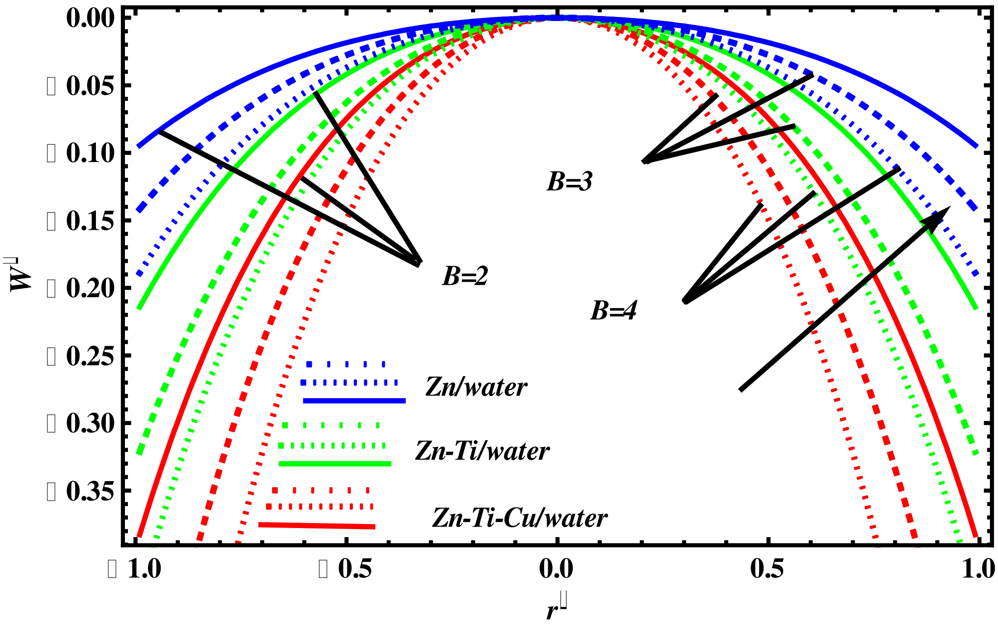

Fig 3(a)

$\mathcal{Z}$˘=0.1, M=2, B_i=0.4, L=0.1, G_r=0.2, E_1=1.5, E_2=1.5, E_3=1.0

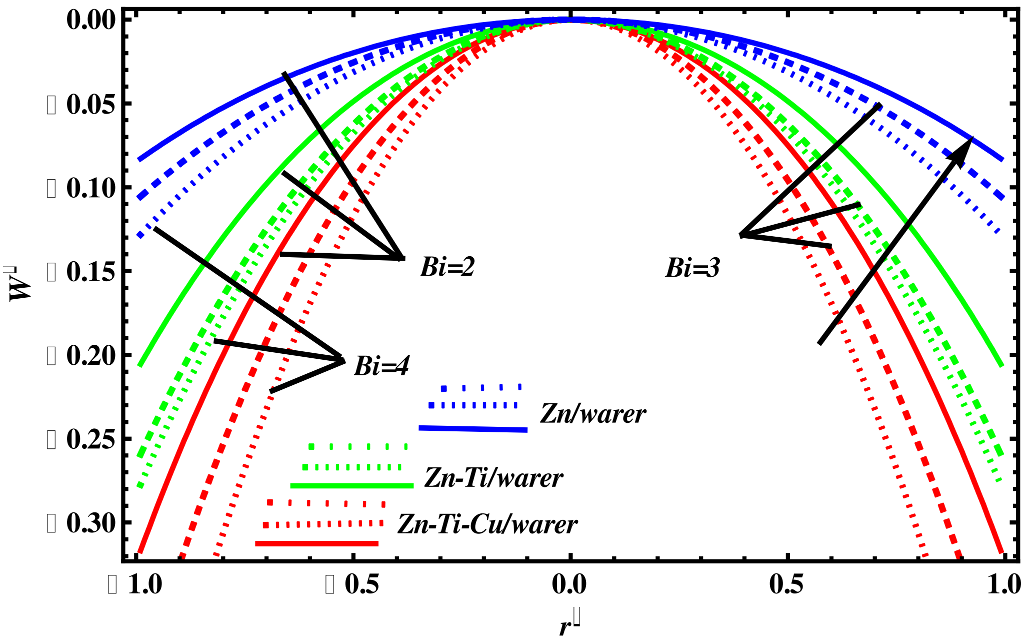

Fig 3(b)

$\breve{\mathcal{Z}}=0.1$, M=2, B=1.0, L=0.2, $G_r=0.4$, $E_1=1.5$, $E_2=1.5$, $E_3=1.0$

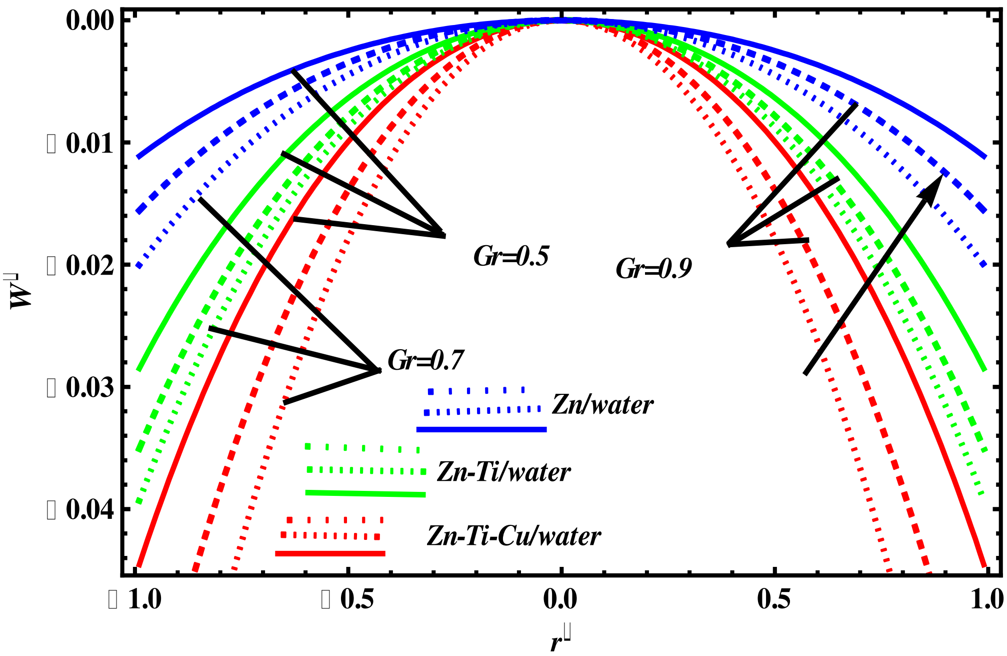

Fig 3(c)

$\breve{\mathcal{Z}}=0.1$, B=0.4, $B_i=0.3$, L=0.2, M=2, $E_1=1.5$, $E_2=1.5$, $E_3=1.0$

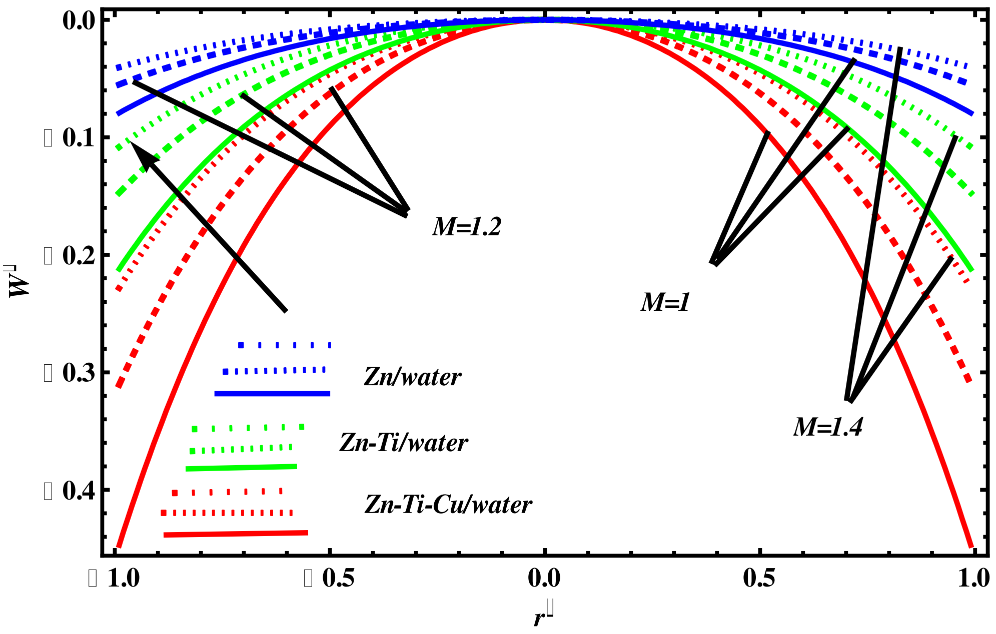

Fig 3(d)

$\breve{\mathcal{Z}}=0.1$, B=3, Bi=0.3, L=0.2, $G_r=0.2$, $E_1=1.5$, $E_2=1.5$, $E_3=1.0$

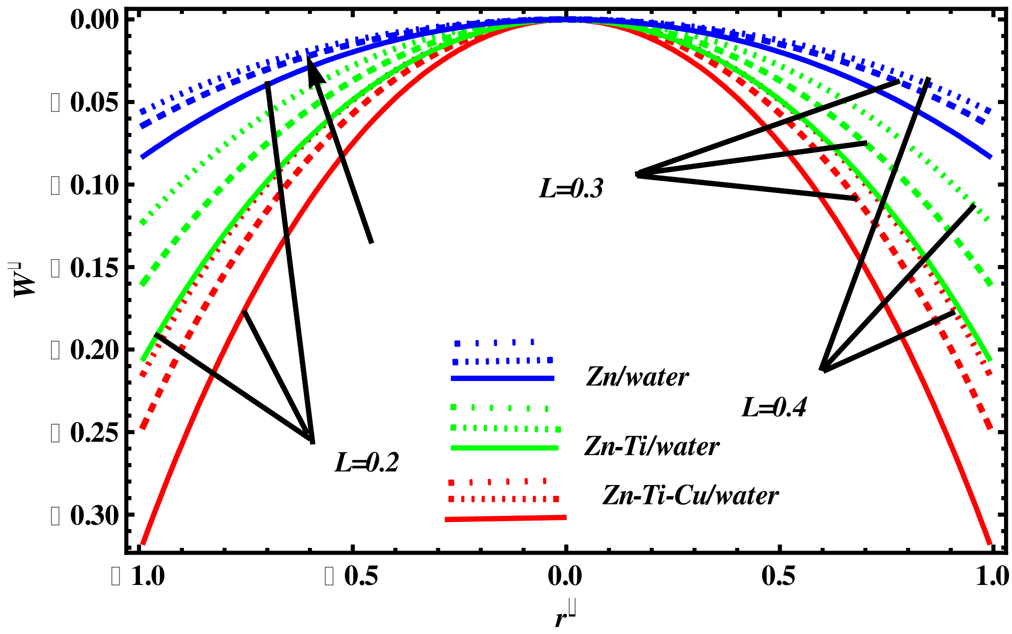

Fig 3(e)

$\breve{\mathcal{Z}}=0.1$, B=3, Bi=0.3, M=2, $G_r=0.2$, $E_1=1.5$, $E_2=1.5$, $E_3=1.0$

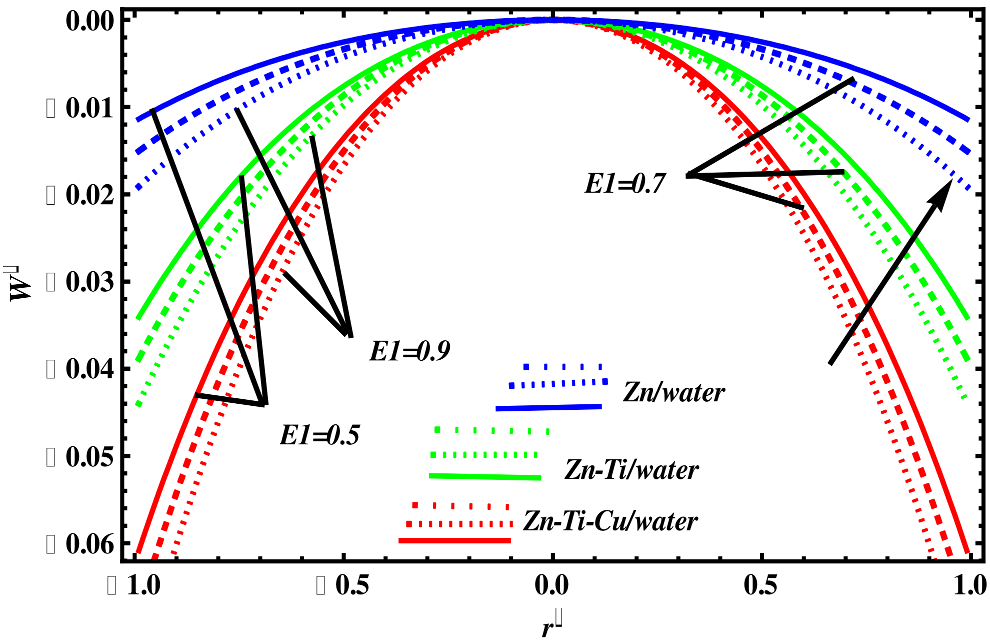

Fig 3(f)

$\breve{\mathcal{Z}}=0.1$, $\boldsymbol{\lambda}=1.2$, $G_r=0.5$, B=0.4, Bi=0.1, M=1.7, $E_3=1.0$, $E_2=1.5$

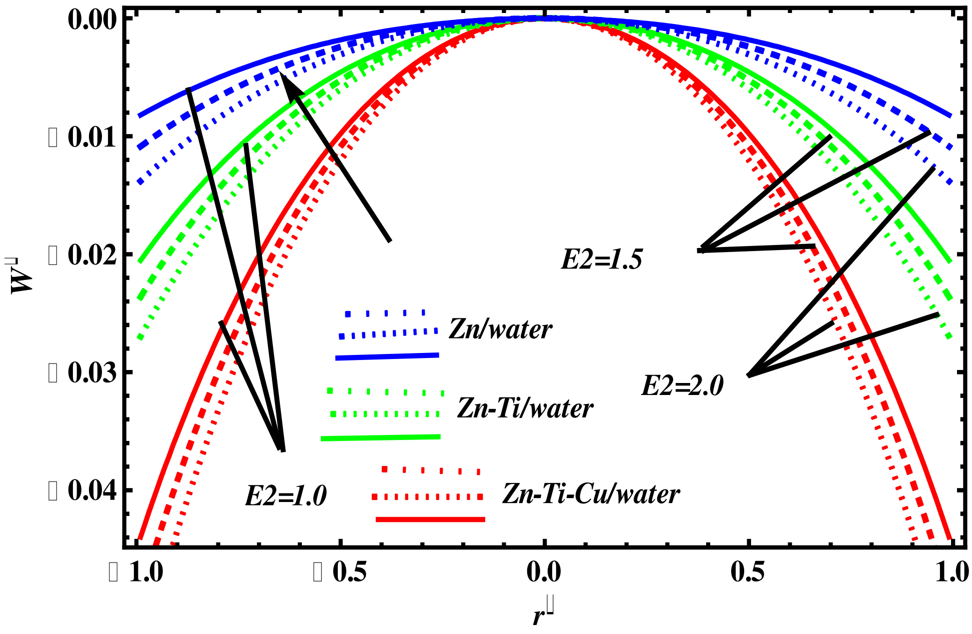

Fig 3(g)

$\breve{\mathcal{Z}}=0.1$, $\boldsymbol{\lambda}=1.2$, $G_r=0.5$, B=0.4, Bi=0.1, M=1.7, $E_1=0.5$, $E_3=2$

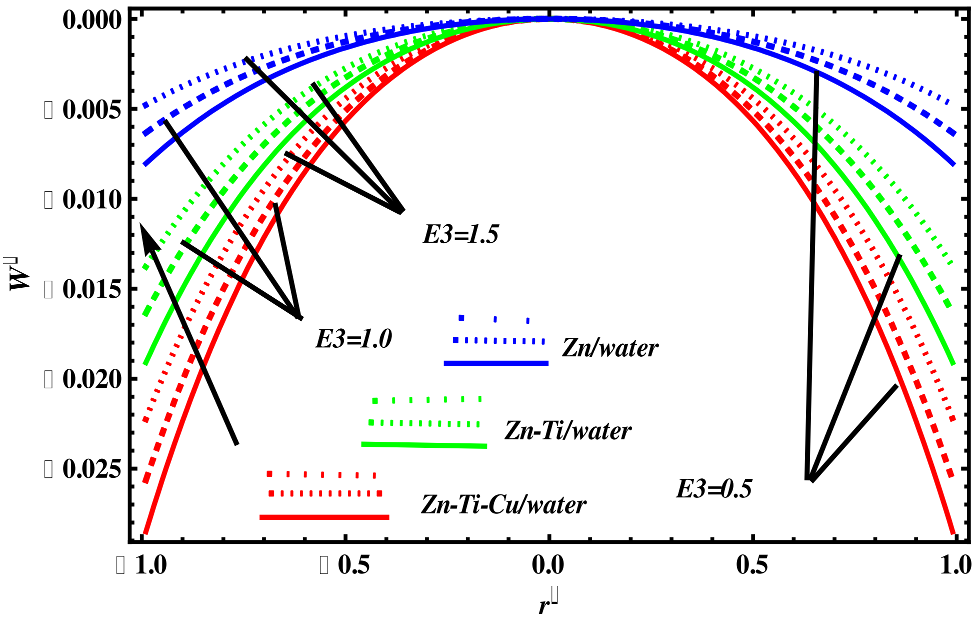

Fig 3(h)

$\mathcal{Z}$=0.1, $\boldsymbol{\lambda}$=1.2, G_r=0.5, B=0.4, Bi=0.1, M=1.7, E_1=1.0, E_2=1.5

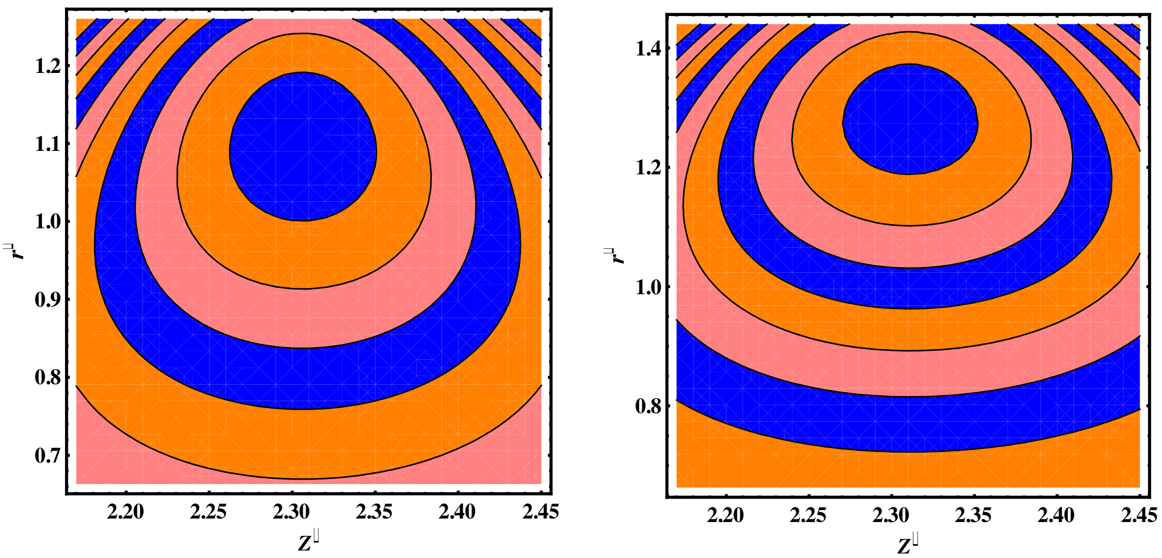

(a) **(b)**

Figs. 4(a-b), Configuration of (Zn-Ti-Cu) /water through a tube for

(i) L (Slip parameter) L=1.0, 1.3 (ii) $\varphi_1 = 0.6, \varphi_2 = 0.6, \varphi_3 = 0.6$

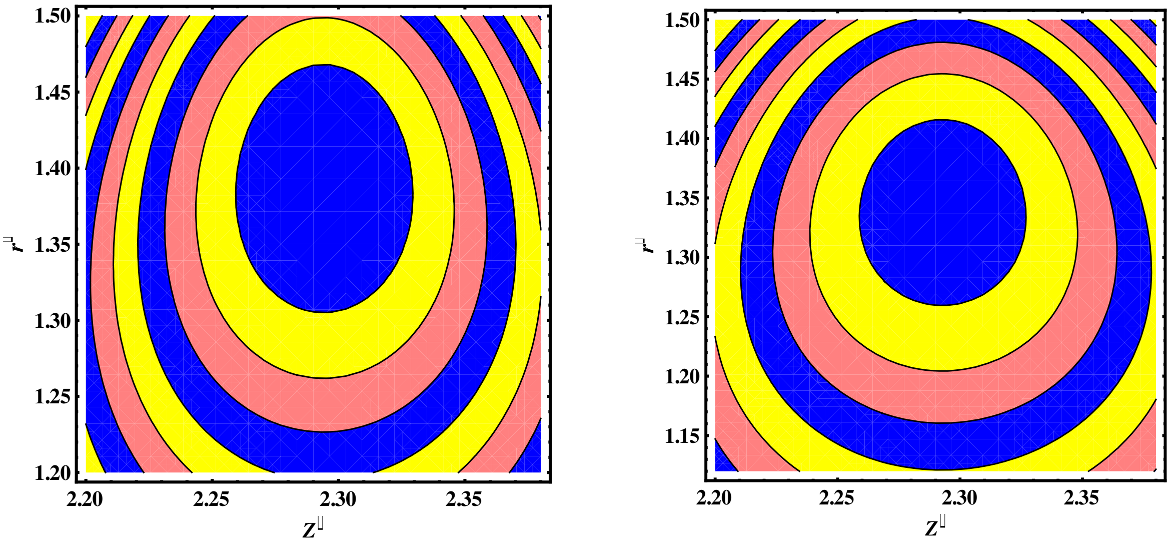

(C) **(d)**

Figs. 4(c-d), Configuration of (Zn-Ti) /water through a tube for

(i) L (Slip parameter) L=1.0, 1.3 (ii) $\varphi_1 = 0.6, \varphi_2 = 0.6, \varphi_3 = 0.0$

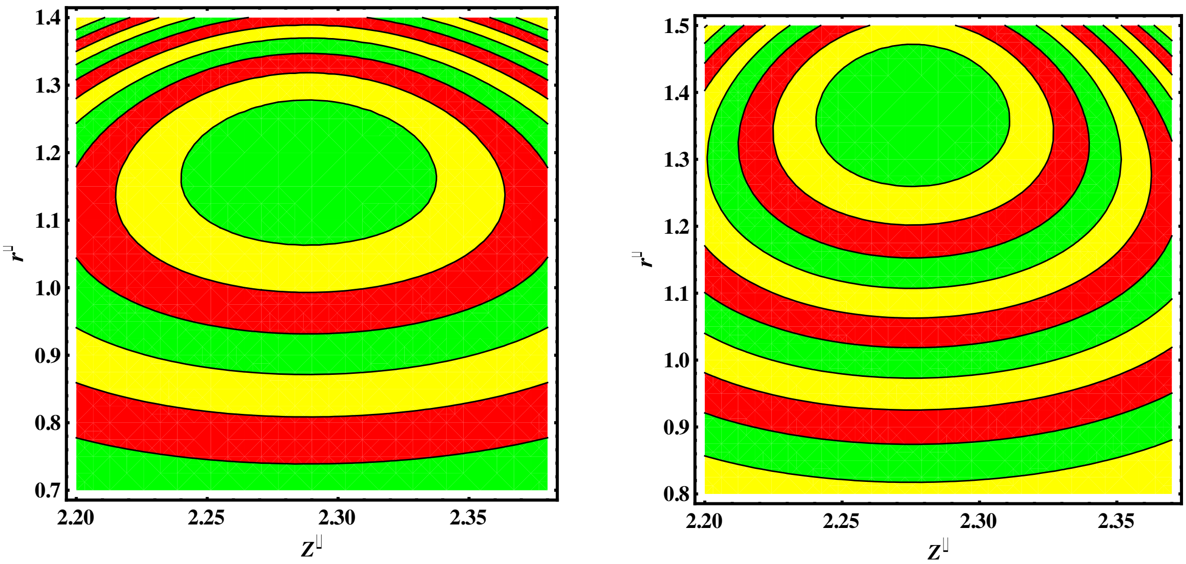

(e) **(f)**

Figs. 4(e-f), Configuration of (Zn) /water through a tube for

(i) L (Slip parameter) L=1.0, 1.3 (ii) $\varphi_1 = 0.6, \varphi_2 = 0.0, \varphi_3 = 0.0$

Results assessment and discussion

This unit marks the physical explanation of the performance of the parameters which rise in the flow field. Fig. 2 is designed to see the impact of heat transfer for nano fluid, hybrid nano fluid and modified nano fluid for different shape effects. It is seen here greater heat transfer curve is observed for Zn-Ti-Cu/water. Less heat transfer is observed for Zn-water. It is seen here high thermal conductivity is detected for modified hybrid nano fluid. Fig. 2a-2c is portrayed to see the effect of heat absorption parameter, biot number, different nano shape effects on temperature profile for nano fluid, hybrid nanofluid and modified nano fluid. It is observed from Fig 2a, that temperature profile increased in the middle of the tube $-0.52 \leq r' \leq 0.5$ whereas it gets opposite behavior near the peristaltic walls. Here, one can observe maximum curve is obtained for Zn-water. Temperature profile for increasing values of the Biot number is depicted in Fig. 2b. As augmented in Biot number, improvement in temperature distribution is seen. Fig. 2c is presented to observe the different nano shape effect for nano, hybrid nano and modified nano fluid on temperature profile. By keeping fixed m=3.7, maximum temperature is found for the nano fluid, and minimum temperature is depicted for modified nano fluid. Same results are revealed for cylinders and platelets shape nanoparticles. Velocity profile for different parameters e.g Heat absorption, Biot number, Grashof number, Magnetic number, velocity slip parameter, Rigidity parameter, Stiffness parameter, Viscous damping force parameter is depicted in Fig 3a-3h. Fig. 3a is designed to see the impact of velocity profile for heat absorption parameter. It is depicted in this Fig velocity curve increased throughout the entire domain when we compare nanofluid, hybrid nano fluid and modified nano fluid. Maximum curve is shown for nano fluid and minimum curve is depicted for modified hybrid nano fluid. But if we increased heat absorption parameter velocity curve decreases for all three types of the nano fluid. From Fig. 3(b) it is observed that for fixed number of Biot number maximum curve is seen for zn-water. For the particular nanofluid case the velocity of the fluid decreases. It is owing to the fact that Biot number decreases the heat transfer rate in the cylinder walls. Same results are shown for hybrid as well as modified nano fluid. Grashof number impact is observed in Fig. 3c. If we fixed Grashof number larger curve is obtained for nanofluid and lessen curve is found for modified hybrid nano fluid. For special cases for example nano fluid increasing the Grashof number decreases the fluid velocity. It is owing the fact the viscous forces show the prominent role that's why fluid velocity decreases, more over same results appear for the hybrid and modified hybrid nanofluid. Magnetic number impact on velocity sketch is shown in Fig. 3d. It is observed in this Fig that velocity profile enhances throughout the entire domain. Velocity slip impact on velocity sketch is depicted in Fig 3e, which shows positive influence on the velocity profile. Rigidity parameter impact on velocity prole is depicted in Fig. 3f. If we fixed E_1 Zn-water showed the larger curve and modified hybrid nanofluid showed the minimum curve, whereas for increasing values of rigidity parameter velocity curve decreases. This is owing to the fact that more resistance is found on the walls. Same results are depicted for stiffness parameter in Fig. 3g. Viscous damping force parameter impact on velocity profile is depicted in Fig 3h. Velocity profile is an increasing function of the viscous damping force parameter. Stream line pattern for velocity slip parameter is portrayed in Fig. 4a-4f. It is shown in these Figs by enhancing slip parameter size of the trapped bolus decreases for modified hybrid nano fluid case, while number of the trapped bolus increases for hybrid case, however size of the trapped boluses decreases for nano fluid case.

Concluding Remarks:

The main points of the considered problem are summarized below

- Temperature curve for Biot number increases throughout the domain.
- Velocity distribution has the curves nanofluid > hybrid nano fluid > modified nano fluid.
- Size of the trapped boluses decreases for modified nano fluid.
- This model is appropriate to the drug dispersal system and also effective for physiological conversion in which nanoparticles have an important role.

References

[1] Michael C, Joseph H S, Kim E B._Pathophysiology, Evaluation, and Management of Chronic Watery Diarrhea. Gastroenterology. 2017;152(3):512-532. doi: 10.1053/j.gastro.2016.10.014.

[2] Latham TW. Fluid motion in a peristaltic pump. Mass: MIII Cambridge MS Thesis. 1966.

[3] Shapiro H, Jaffrin M Y, Weinberg S L. Peristaltic pumping with long wavelengths at low Reynolds number. Journal of Fluid Mechanics. 1969; 37:799–825. doi.org/10.1017/S0022112069000899.

[4] Tripathi D. Study of transient peristaltic heat flow through a finite porous channel. Mathematical and computer Modelling.2013;57(5):1270–83.

[5] Riaz A, Bhatti M M Ellahi R, Zeeshan A, Sait S M. Mathematical analysis on an asymmetrical wavy motion of blood under the influence entropy generation with convective boundary conditions. Symmetry. 2020;12(1):102. doi.org/10.3390/sym12010102

[6] Ellahi R, Bhatti M M, Vafai K. Effects of heat and mass transfer on peristaltic flow in a non-uniform rectangular duct. International Journal of Heat and Mass Transfer. 2014; 17:706-719. doi.org/10.1016/j.ijheatmasstransfer.2013.12.038

[7] Hayat T, Zahir H, Mustafa M, Alsaedi A. Peristaltic flow of Sutterby fluid in a vertical channel with radiative heat transfer and complaint walls: a numerical study. Results in Physics. 2016; 6:805–810.

[8] Fusi L, Farina A. Peristaltic axisymmetric flow of a Bingham fluid. Applied Mathematics and Computation. 2018; 320:1–15. doi:10.1016/j.amc.2017.09.017.

[9] Abbasi FM, Hayat T, Ahmad B. Peristaltic transport of copper–water nanofluid saturating porous medium. Physica E Low-dimensional Systems and Nanostructures. 2015; 67:47–53. DOI:10.1016/j.physe.2014.11.002

[10] Akbar NS, Butt AW. Ferromagnetic effects for peristaltic flow of Cu–water nanofluid for different shapes of nanosize particles. Applied Nanoscience. 2016; 6:379–85.

[11] Mekheimer KH, Hasona WM, Abo-Elkhair RE, Zaher AZ. Peristaltic blood flow with gold nanoparticles as a third grade nanofluid in catheter: application of cancer therapy. Physics Letter A. 2018; 382:85–93. doi.org/10.1016/j.physleta.2017.10.042

[12] MosayebidorchehS Hatami M. Analytical investigation of peristaltic nanofluid flow and heat transfer in an asymmetric wavy wall channel (part 1: straight channel). International

Journal of Heat and Mass Transfer. 2018; 126:790
doi:10.1016/j.ijheatmasstransfer.2018.05.080

[13] Farooq S, Khan MI, Waqas M, Hayat T, Alsaedi A. Peristalsis of carbon nanotubes with radiative heat flux. Appl Nanosci. 2020;10(2):347–57. doi. 10.1007/s13204-019-01148-5.

[14] Sadaf H, Nadeem S. Fluid Flow analysis of cilia beating in a curved channel in the presence of manetic field and heat transfer. Canadian Journal of Physics. 2020; 98:191–197. doi.org/10.1139/cjp-2018-0715.

[15] Bhatti MM, Abbas MA. Simultaneous effects of slip and MHD on peristaltic blood flow of Jeffery fluid model through a porous medium. Alexandria Engineering Journal. 2016;55(2):1017–1023. doi.org/10.1016/j.aej.2016.03.002

[16] Hayat T, Khan AA, Bibi F, Farooq S. Activation energy and non-Darcy resistance in magneto peristalsis of Jeffery material Journal of Physics and Chemistry of Solids. 2019; 129:155–61. doi:10.1016/j.jpcs.2018.12.044.

[17] Farooq S, Khan MI, Waqas M, Alsaedi A. Theoretical investigation of peristalsis transport in flow of hyperbolic tangent fluid with slip effects and chemical reaction. Journal of Molecular Liquids. 2019; 285:314–322. doi.org/10.1016/j.molliq.2019.04.051.

[18] Abo-Elkhair RE, Mekheimer KS, Moawed MA. Combine impacts of Electrokinetic variable viscosity and partial slip on peristaltic MHD flow through a micro-channel. Iranian Journal of Science and Technology. 2019; 43:201–212. doi:10.1007/S40995-017-0374-Y

[19] Farooq S, Khan MI, Waqas M, Alsaedi A. Transport of hybrid type nanomaterials in peristaltic activity of viscous fluid considering nonlinear radiation, entropy generation and slip effects. Computer Methods and Programs in Biomedicine. 2020; 184:105086. doi: 10.1016/j.cmpb.2019.105086.

[20] Saleem S, Mumraiz S, Aamir A et al, Investigation on TiO_2–Cu/H_2O hybrid nanofluid with slip conditions in MHD peristaltic flow of Jeffrey material. Journal of Thermal Analysis and Calorimetry. 2021;143: 1985–1996. doi:10.1007/s10973-020-09648-1.

[21] Dero S, Rohni A M, Saaban A, Khan I et al. Dual solutions and stability analysis of micropolar nanofluid flow with slip effect on stretching/shrinking surfaces. Energies. 2019;12(23), 4529. https://doi.org/10.3390/en12234529.

[22] Fudholi A, Zohri M, Rukman N S. Exergy and sustainability index of photovoltaic thermal (PVT) air collector: A theoretical and experimental study. Renewable and Sustainable Energy Reviews. 2019; 100 (1): 44–51. doi:10.1016/j.rser.2018.10.019.

[23] Amalraj S, Michael PA. Synthesis and characterization of Al2O3 and CuO nanoparticles into nanofluids for solar panel applications. Results in Physics 15 (2019) 102797. doi.org/10.1016/j.rinp.2019.102797.

[24] Sheikholeslami M, Rezaeianjouybari B, Darzi M, Shafee A et al. Application of nano-refrigerant for boiling heat transfer enhancement employing an experimental study, International Journal of Heat and Mass Transfer. 2019; 141: 974-980. doi: 10.1016/j.ijheatmasstransfer.2019.07.043.

[25] Choi S U, Eastman JA, Enhancing thermal conductivity of fluids with nanoparticles (No. ANL/MSD/CP-84938; CONF-951135-29). Argonne National Lab., IL (United States) 1995.

[26] Pak B C, Cho Y I. Hydrodynamic and heat transfer study of dispersed fluids with submicron metallic oxide particles. Experimental Heat Transfer. 1998; 11 (2):151–170. doi.org/10.1080/08916159808946559.

[27] Kefayati G H R. Heat transfer and entropy generation of natural convection on non-Newtonian nanofluids in a porous cavity. Powder Technology. 2016:299;127–149. doi.org/10.1016/j.powtec.2016.05.032.

[28] Mehmood A, Iqbal M S. Heat transfer analysis in natural convection flow of nanofluid past a wavy cone. Journal of Molecular Liquids. 2016; 223:1178–1184. doi.org/10.1016/j.molliq.2016.09.029.

[29] Hashemi H, Namazian Z, Zadeh S M H, Mehryan S A M. MHD natural convection of a micropolar nanofluid flowing inside a radiative porous medium under LTNE condition with an elliptical heat source. Journal of Molecular Liquids. 2018; 217: 914–925. doi: S0167732218328666.

[30] Suresh S., Venkitaraj K.P., Selvakumar P. & Chandrasekar. M. Synthesis of Al2O3–Cu/water hybrid nanofluids using two step method and its thermo physical properties. Colloids and Surfaces A. 2011; 388: 41–48. doi.org10.1016/J.COLSURFA.2011.08.005.

[31] Hayat T, Nadeem S. Heat transfer enhancement with Ag–CuO/water hybrid nanofluid. Results in Physics. 2017; 7:2317–2324. doi.org/10.1016/j.rinp.2017.06.034.

[32] Safaei M R, Hajizadeh, A, Afrand, M. et al. Evaluating the effect of temperature and concentration on the thermal conductivity of ZnO-TiO2/EG hybrid nanofluid using artificial neural network and curve fitting on experimental data. Physica A: Statistical Mechanics and its Applications. 519(C) 209-216. doi: 10.1016/j.physa.2018.12.010

[33] Sulochana C, Ashwinkumar G P. Impact of Brownian moment and thermophoresis on magnetohydrodynamic flow of magnetic nanofluid past an elongated sheet in the presence of

thermal diffusion. Multidiscipline Modeling in Materials and Structures. 2018: 14 (21); doi:10.1108/MMMS-12-2017-0168.

[34] Nadeem S, Nadeem A. Effects of MHD on Modified Nanofluid Model with Variable Viscosity in a Porous Medium. Nanofluid Flow in Porous Media. 2019 doi:10.5772/intechopen.84266.